European Journal of Pharmacology 962 (2024) 176216

Contents lists available at ScienceDirect

European Journal of Pharmacology

journal homepage: www.elsevier.com/locate/ejphar

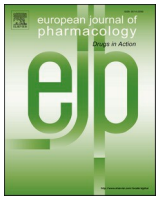

Edoxaban treatment in a post-infarction experimental model

Javier Martínez-Fernández [a,b,1], Cristina Almengló [b,1], Borja Babarro [b], Ramón Iglesias-Rey [c], Tomás García-Caballero [b,d], Ángel L. Fernández [e,g], Miguel Souto-Bayarri [a,b], José R. González-Juanatey [b,f,g,i], Ezequiel Álvarez [b,g,h,*]

[a] Servicio de Radiología, Complexo Hospitalario Universitario de Santiago de Compostela, Santiago de Compostela, Spain
[b] Instituto de Investigación Sanitaria de Santiago de Compostela (IDIS), Complexo Hospitalario Universitario de Santiago de Compostela (CHUS). SERGAS, Travesía da Choupana s/n, A Coruña, Santiago de Compostela, 15706, Spain
[c] Neuroimaging and Biotechnology Laboratory (NOBEL), Clinical Neurosciences Research Laboratory (LINC), Instituto de Investigación Sanitaria de Santiago de Compostela (IDIS), Complexo Hospitalario Universitario de Santiago de Compostela (CHUS), SERGAS, Travesía da Choupana s/n, A Coruña, Santiago de Compostela, 15706, Spain
[d] Department of Morphological Sciences, School of Medicine, University of Santiago de Compostela and University Clinical Hospital, 15782, Santiago de Compostela, Spain
[e] Heart Surgery Department, University Hospital of Santiago de Compostela, Santiago de Compostela, Spain
[f] Departamento de Medicina, Universidad de Santiago de Compostela, 15782, A Coruña, Spain
[g] CIBERCV, Madrid, Spain
[h] Departamento de Farmacología, Farmacia y Tecnología Farmacéutica, Universidad de Santiago de Compostela, 15782, Santiago de Compostela, A Coruña, Spain
[i] Servicio de Cardiología y Unidad de Hemodinámica. Complexo Hospitalario Universitario de Santiago de Compostela (CHUS). SERGAS, Travesía da Choupana s/n, A Coruña, Santiago de Compostela, 15706, Spain

ARTICLE INFO

Keywords:
Edoxaban
Acute myocardial infarction experimental model
Cardiac remodelling after infarction
Cardiac magnetic resonance imaging
Post-infarction anticoagulant treatment

ABSTRACT

Background: The sequelae of myocardial infarction (MI) require specific pharmacological therapy to minimise the post-MI remodelling, which in many cases evolves into cardiovascular complications. The aim of this study was to analyse the effect of edoxaban, an oral anticoagulant, on cardiac recovery in a rat model of permanent coronary artery ligation.
Methods: An experimental method to assess the post-MI remodelling in rats for 4 weeks, based on cardiac magnetic resonance imaging (MRI) and final histological analysis of the hearts was performed. The influence of daily oral treatment with edoxaban (20 mg/kg/day) for 28 days post-MI was analysed in comparison to vehicle.
Results: In our model, edoxaban was shown to be safe and bleeding was observed in 1 of 10 animals. General physical recovery of the treated animals was shown by higher body weight recovery compared with non-treated animals (38.6 ± 2.9 vs. 29.9 ± 3.1 g, respectively, after 28 days). There was not a pronounced effect of edoxaban in post-MI cardiac remodelling, but mitigated fibrosis was observed by the reduced expression of vascular endothelial growth factor and tumour growth factor β1 in the peri-infarct zone.
Conclusions: Our analysis provided the experimental basis to support the feasibility of MRI to study cardiac function and characterise myocardial scarring in a rat model. Overall data suggested the safety of edoxaban in the model, and compared to placebo, it showed a better post-MI recovery, probably by reducing fibrosis of the heart. Further research on mid-term cardiac recovery with edoxaban after MI is justified.

1. Introduction

Cardiovascular disease is the leading cause of death globally and the leading cause of premature death in Europe, and ischaemic heart disease is its most important subgroup (World Health Organization, 2020). Acute myocardial infarction (AMI) survival has improved because of diagnostic and therapeutical advances (Keeley et al., 2003; Kim et al., 2008); with a subsequent increment of morbidity and health

* Corresponding author. Instituto de Investigación Sanitaria de Santiago de Compostela (IDIS), Complexo Hospitalario Universitario de Santiago de Compostela (CHUS). SERGAS, Travesía da Choupana s/n, A Coruña, Santiago de Compostela, 15706, Spain.
E-mail address: ezequiel.alvarez@usc.es (E. Álvarez).
[1] These authors contributed equally to this work and share first authorship.

https://doi.org/10.1016/j.ejphar.2023.176216
Received 28 July 2023; Received in revised form 4 November 2023; Accepted 16 November 2023
Available online 29 November 2023

expenditure (Ahmed et al., 2012; Klocke et al., 2007). Left ventricular dysfunction due to adverse remodelling is the most important predictor of poor outcomes (including death, recurrent myocardial infarction, heart failure, arrhythmias, angina, and stroke), and it is crucial to prevent it in an early stage (Ahmed et al., 2012; Li et al., 2019). In this field, our challenges are to understand the underlying pathophysiological mechanisms of this process, identify and test novel therapeutic approaches, and translate this knowledge to clinical practice (Li et al., 2019; Malliaras et al., 2013).

Bearing in mind that it has been suggested that after the acute phase of coronary syndromes, the hypercoagulable state is maintained for a time (Ardissino et al., 2003; Orbe et al., 2008), anticoagulation after AMI for secondary prevention is a therapeutic option, and this includes the direct oral anticoagulants (DOACs) (Sharma et al., 2014). DOACs are considered an interesting, safe, and efficient alternative to old vitamin K antagonists in several clinical settings (Capodanno et al., 2020; Fawzy et al., 2019; Makam et al., 2018). In particular, factor X-activated (FXa) inhibitors have been shown to reduce stroke or systemic embolism, as well as all-cause mortality in patients with atrial fibrillation (Deitelzweig et al., 2022). However, their effect on acute coronary syndrome prevention is less clear (Pop et al., 2019). Nevertheless, in a sub-analysis of the ENGAGE AF-TIMI 48 trial, the reduction in ischaemic events with edoxaban *versus* warfarin was greater in patients with established coronary artery disease, while bleeding was significantly reduced with edoxaban regardless of coronary artery disease status (Zelniker et al., 2019). Apart from secondary prevention, DOACs could also modulate the pathophysiological mechanisms after AMI survival, particularly in the cardiac remodelling process that always starts after an infarction. In this sense, edoxaban has shown pleiotropic effects on vascular cells that could improve myocardial recovery after ischaemia (Almenglo et al., 2020). This is a new hypothesis, but considering that the myocardial infarction event rates continue to increase as the population ages (Khan et al., 2020), it is imperative to maintain policies to reduce cardiovascular risk factors and to explore new approaches to myocardial infarction treatment. One of these approaches is to reduce adverse cardiac remodelling after infarction, and we will test the possible role of edoxaban in this setting.

Preclinical data about the effects of DOACs in this particular post-infarction setting should be provided. Therefore, creating suitable animal experimentation models plays an essential role in those advances (Do et al., 2018; Klocke et al., 2007; Shudo et al., 2011). However, one of the limitations of these models, especially in small animals, is the use of advanced cardiac imaging techniques. In this study, we have chosen the rat because of its ease of management and its relatively few ethical problems (Klocke et al., 2007). We chose cardiac magnetic resonance imaging (MRI) because it is the *Gold Standard* technique in clinical practice for comprehensive evaluation of patients with cardiac ischaemic diseases (Ahmed et al., 2012; Kim et al., 2008; Ordovas and Higgins, 2011). This technique is constantly evolving with new sequences to explore various aspects of the disease (Do et al., 2018; Garg et al., 2018; Yla-Herttuala et al., 2018). In summary, the objective of the study was to analyse the possible influence of edoxaban in the post-infarction myocardial remodelling in a rat experimental model of permanent coronary ligation, functionally characterised by cardiac MRI during the process, and histologically analysed as the end-point measurement. The progress of this objective could open new therapeutic alternatives for myocardial infarction and the protection of cardiac tissue, with drugs and molecular mechanisms not yet explored in this regard. This, ultimately, would contribute to reducing the socio-sanitary burden of ischaemic heart disease.

2. Materials and methods

2.1. Animals, invasive procedures and postoperative care

The entire study and protocols were approved by the Bioethics Committee of the University of Santiago de Compostela and the regional Galician Government (code 15,005/16/004).

Twenty-two male Wistar-Kyoto rats (weight 350 ± 50 g; from the central animal facility, Santiago de Compostela) were divided into an intervention group (IG; $n = 18$) and a control group (CG, sham; $n = 4$). In the IG, a surgical ligation of the left anterior descending (LAD) artery of the heart was performed to create an AMI, following the procedure described by Pfeffer et al. with slight modifications (Pfeffer et al., 1979). In brief, animals were anesthetised with 60 mg/kg of ketamine and 5 mg/kg of xylazine. A toe and tail pinch confirmed sedation. Then, a catheter was inserted into the trachea and connected to a ventilator that introduced anaesthesia from an induction chamber with 3% isoflurane and oxygen for 5–7 min. Anaesthesia was sustained afterwards with 2.5% isoflurane and oxygen at a ventilation rate of 2.5 l/min. Animals were placed in the right decubitus position on a warming pad at 37 °C, and the left lateral surface of the chest was shaved and disinfected. The depth of anaesthesia was continually monitored by assessment of the tail-pinch reflex and respiratory rhythm. Following a left thoracotomy in the fourth intercostal space and the application of a chest retractor, the pericardium was dissected and the LAD artery was ligated 1–2 mm below the left auricular appendage with a 6/0 polypropylene thread (Prolene 6/0; Ethicon Inc., Johnson & Johnson, New Brunswick, NJ, US) in animals of the IG, whereas animals of the CG were closed as follows, without ligation. The chest retractor was retired, and the intercostal space and chest skin were sutured with 4/0 Vicryl thread (Vicryl v496 h, 4/0 Ethicon Inc.). A cannula was left between the sutures that allowed intrathoracic air to be aspirated once the wound was closed, and it was removed immediately after this manoeuvre. Finally, the ventilator was turned off and removed when the animal was able to breathe on its own. The researchers took all possible measures to minimise animals' pain and suffering. Buprenorphine (0.1−2.5 mg/kg) was injected s. c. 20–30 min before the beginning of the anaesthesia and immediately before the end of the surgery as postoperative analgesia.

After surgery, animals were kept separately in a cage warmed with a heat lamp until they had fully recovered from anaesthesia. Welfare monitoring of animals via behavioural observation was performed every day. Food (pellets) and fresh water were provided *ad libitum*. A 12 h: 12 h light: dark cycle and a constant temperature of 24 °C were maintained during the entire experimentation time. At the end of the study, animals were humanely killed. Exsanguination was performed under general anaesthesia (isoflurane 2.5% in oxygen at 2.5 l/min), the thorax was opened, blood was withdrawn from the vena cava, and the heart was harvested.

2.2. Magnetic resonance imaging

MRI procedures were performed under sevoflurane anaesthesia (5% induction and 3.5% maintenance in a gas mixture of 70% NO_2 and 30% O_2) and breath monitoring. During MRI studies, each animal was fixed in a Plexiglas holder using a tooth bar, ear bars and adhesive tape to minimise spontaneous movement during imaging acquisition. Each animal underwent 3 MRI studies: basal (MRI0), 4 days (MRI1) and 4 weeks (MRI2) after the AMI onset. All cardiac MRI studies (CMR) were performed on a 9.4 T horizontal bore magnet (Bruker BioSpin, Ettlingen, Germany) with 440 mT/m gradients and a quadrature volume coil (7 cm in diameter).

The study protocol consisted of covering the entire heart with Gradient echo (GE) cine MR images with electrocardiogram triggering in the prone position in the short axis (SA, for heart function quantification purposes). A single long-axis slice was obtained in order to place the corresponding short-axis slices covering the apex to the base (8–10 slices). GE sequence was used to acquire cine cardiac images with the following parameters: echo time (TE) = 3.3 ms, repetition time (TR) = 8 ms, slice thickness 1.5 mm, no slice separation, field of view (FOV) = 60 × 60 mm^2, matrix size 256 × 256 (isotropic in-plane resolution of 0.234 mm/pixel). Sixteen cine-frames were recorded to cover the cardiac

cycle. The presence of delayed myocardial enhancement was assessed with late gadolinium enhancement (LGE) sequence after intravenous injection of a dose of 0.5 mmol/kg body weight Gd-DTPA. For this purpose, a fast low-angle shot pulse (IR-FLASH) was used. Short-axis views were obtained using the following imaging parameters: repetition time, 430 ms; echo time, 2.1 ms; interpolated in-plane resolution, 0.313 × 0.313 mm; slice thickness, 1.5 mm with contiguous 6 slices; inversion time, 350–450 ms. Inversion time was optimised to the null point of normal myocardium manually in each individual, and a cardiac gating system was used in IR-FLASH sequences. The total acquisition time was 90 min.

Data were collected by a radiologist with more than 15 years of experience in CMR. The following parameters were quantified for the left ventricle (LV): end-diastolic volume (EDV), end-systolic volume (ESV), and ejection fraction (EF). Calculations were completed from the cine MR sequences on SA planes. The volumes of all LV slices in maximum relaxation and end-contraction stages were calculated to obtain EDV and ESV, respectively. EF was calculated as a ratio (%) according to the expression: EF = (EDV-ESV)/EDVx100.

The criteria followed for LV measurements are detailed as follows. Baseline slices, near the valve plane, were revised carefully to not include the left atrium. Papillary muscles and trabeculae were included in volume and EF calculations as part of the cavity because it assures lower interoperator variability. Global LV function was quantified using Segment v2.0 R5165 (http://segment.heiberg.se) (Heiberg et al., 2010). Expert manual drawing of ventricular images was performed since it was considered the reference standard in practice.

Abnormalities (late enhancement) in the LGE sequence to assess myocardial scarring were analysed in a semi-quantitative visual assessment scale, using the following categories: 'No', 'Possible', 'Probable' and 'Yes', in increasing order of suspicion of pathology. The categorisation was made by consensus between two radiologists.

2.3. Edoxaban treatment

After the MRI1, AMI was confirmed, and the animals in the IG were divided randomly into treated (TG) and non-treated (NTG) groups. The day after MRI1, treatment started in the TG by oral administration of edoxaban 20 mg/kg by the intragastric gavage technique from a 3 mg/mL solution of edoxaban in water (this corresponds with 0.66 ml/100 g of body weight). The NTG was subjected to the same intragastric gavage technique, but water, at the same volume as in TG, was administrated instead of edoxaban. Administrations were done daily, always at the same time of the day (9–11 *a.m.*) until the day of the last MRI (MRI2) and sacrifice of the animal (completing 28 days of treatment and follow-up). Attention to external signs of bleeding (in the nose, eyes, nails, blood in the animal bedding, etc.) was paid to detect any increase in bleeding risk as soon as possible.

2.4. Histological analysis

Rats were sacrificed 28 days post-surgery and their hearts were harvested for histological studies. Animal and heart weights were recorded. Hearts were fixed in 4% paraformaldehyde-buffered solution, pH = 7 (Alfa Aesar, Avantor, Radnor, PA, US), for 24 h at room temperature. Hearts were then bisected and dehydrated, through a series of ethanol and xylene and embedded in paraffin. Four blocks of paraffin were done for each heart, and the blocks were done by four equal short-axis slides of 0.5 cm each. Sections of 4 μm thick were mounted on silanised coated slides (Dako-Agilent, Santa Clara, CA). Epitope retrieval was performed in a PT-Link (Dako-Agilent) at high pH for 20 min and then automatically immunostained in an Autostainer-Link 48 (Dako-Agilent), employing the monoclonal antibodies and protocols listed in Table 1. As a detection system, we used EnVision FLEX/HRP (Dako-Agilent), for 30 min, and 3,3′-diaminobenzidine tetra-hydrochloride (DAB) as the chromogen for 10 min. The following proteins were immunohistochemically detected: desmin, vimentin, α-smooth muscle actin (α-SMA), vascular endothelial growth factor (VEGF), metalloprotease 9 (MMP9), tissue inhibitor of metalloproteinases 1 (TIMP1), superoxide dismutase 2 (SOD2), and tumour growth factor beta1 (TGFβ1). For haematoxylin–eosin (HE) and Masson trichrome staining standard protocols were used.

Table 1
Antibodies and incubation protocols.

Antigen	Antibody's Source	Clone	Catalogue No. & Manufacturer	Conc.	Incubation time
SOD2/Mn	Mouse	349,810	MAB3419, R&D Systems	1:500	20 min
MMP-9	Mouse	4H3	MAB911, R&D Systems	1:20	20 min
TIMP-1	Mouse	63,515	MAB970, R&D Systems	1:100	20 min
VEGF	Mouse	VG1	MA1-16629, ThermoFisher	1:20	20 min
TGF-β1	Mouse	1,018,746	MAB10502, R&D Systems	1:5000	20 min
Vimentin	Mouse	V9	M0725, Dako-Agilent	RTU	20 min
α-SMA	Mouse	1A4	M0851, Dako-Agilent	RTU	20 min
Desmin	Mouse	D33	M0760, Dako-Agilent	RTU	20 min

Abbreviations: α-SMA: α-smooth muscle actin; Conc.: concentration; MMP-9: metalloprotease 9; RTU: ready to use; SOD2: superoxide dismutase 2; TGF-β1: tumour growth factor beta1; TIMP1: tissue inhibitor of metalloproteinases 1; VEGF: vascular endothelial growth factor.

Images of transversal sections of hearts were captured with a loupe Leica DMD 108 (Leica). We used the slice where the scar was largest to assess the AMI as scarred/total LV area, expressed in a percentage. Immunohistochemistry quantification was performed using the 'Split channels' function (green channel) from Fiji-ImageJ® software (https://imagej.net/software/fiji/). For each measurement, at least $n = 3$ samples were used for the histologic experiments.

2.5. Data analysis

The statistical analyses were performed with SPSS (Statistical Package for the Social Sciences), version 17.0. The categorical or dichotomous variables were expressed as absolute values and percentages and were compared with the Pearson χ^2 test. In the case of continuous variables, normality was checked with the Kolmogorov–Smirnov test. When normally distributed, variables were described as the mean ± standard error of the mean (s.e.m), and when not, as the median and inter-quartile range. The Student's *t*-test was used for the comparisons of continuous variables between groups of patients (two-tail distribution and equal variances between samples) when variables fulfilled the condition of normality, whereas the Mann–Whitney *U* test was used when variables did not fulfil the condition of normality. Non-normal distributed variables were compared with the Wilcoxon test. A *p*-value of <0.05 was considered statistically significant.

3. Results

3.1. Interventional procedure and treatment

Forty-seven rats were included in the study. Two of them were excluded before starting the interventional programme after they did not pass the routine health tests in the animal facility, nineteen died during the surgery (intraoperative mortality of 42.2%), three more did not survive to the first 6 h after surgery (perioperative mortality of 48.9%), and one more died during the 4-week follow-up period by internal bleeding (day 5 of edoxaban's administration, overall mortality

51.1%). Therefore, 22 animals survived until histological analysis, from which four were sham-operated (Fig. 1). In the IG, nine rats of the TG were treated with oral edoxaban (20 mg/kg daily) for 28 days. In parallel, nine rats were included in the NTG and administered water in the same quantity as the TG (6.66 mL/kg daily) by the intragastric gavage technique. One extra-animal was included in the TG that died of internal bleeding after day 5 of edoxaban administration. Anatomic analysis after death suggested that an injury to the oesophagus or stomach during the intragastric gavage technique caused gastrointestinal bleeding that the anticoagulant effect of edoxaban did not stop. No other signs of bleeding were observed in the rest of the animals used in the study, so it was not justified to conduct blood sampling during the period of edoxaban treatment to monitor clotting times.

3.2. Post-infarction period

After the surgery to provoke the AMI, the animals showed a general recovery observed by their physical activity and body weight recovery. Animals from the NTG weighting 362.4 ± 14.2 g on the day of the surgery increased a mean of 29.9 ± 3.1 g after 28 days of water administration (vehicle of edoxaban). On the other hand, the animals from the TG (358.1 ± 15.0 g on the day of the surgery) gained a mean of 38.6 ± 2.9 g, being statistically significant in comparison with the NTG ($p = 0.047$, Mann–Whitney U). This weight recovery tended to be higher in the TG than in the NTG from the day 11 of treatment, being statistically significant in the last days of treatment (Fig. 2). The sham group gradually increased their body weight after the thoracic surgery, but two differences were appreciated in comparison with the NTG and TG. First, rats did not suffer a myocardial infarction, so the impact of the surgery was less pronounced than in the other groups in terms of body weight loss and behaviour in the days after the intervention and before starting the treatment (data not shown). After recovery from the anaesthesia, the animals showed normal behaviour without signs of pain and normal access to food and water. Second, the body weight gain continued during the following 28 days, but it was more gradual than in the case of the other two groups (21.7 ± 3.1 g, $p = 0.024$ and $p = 0.001$ with respect to the NTG and TG, respectively; Fig. 2).

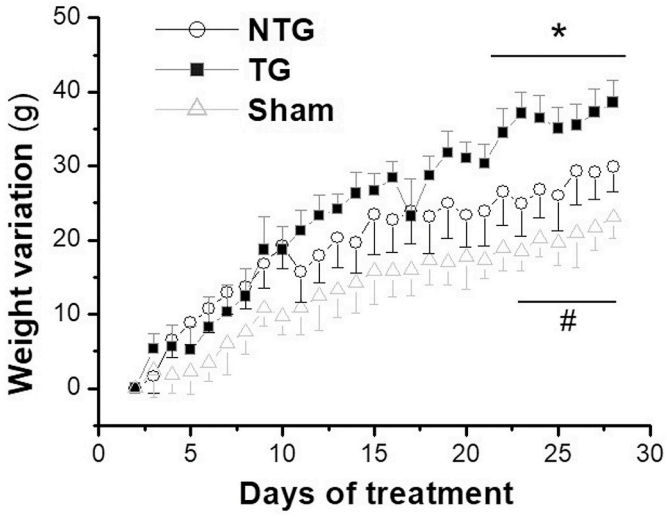

Fig. 2. Weight recovery after infarction. Weight variation during the treatment time for the non-treated group (NTG, placebo), the treated group (TG) with edoxaban (20 mg/kg/day), and sham group (thoracic surgery without infarction induction). Points represent the mean values of the weight variation with respect to the first day of treatment for all the animals in the same group. Vertical bars show the standard error of the mean for each value. *$p < 0.05$ between NTG and TG; #p < 0.05 between Sham and NTG.

3.3. MRI, infarction confirmation and cardiac remodelling follow-up

Table 2 summarizes the data from the MRI at the different times and groups. No significant differences were found between the NTG and TG regarding the EDV, ESV, SV, EF or estimated LV mass over the study. AMI induced a reduction of the EDV, which was recovered during the post-infarction follow-up in both the NTG and TG, with a mean overall increase of 0.07 and 0.13 mL (for NTG and TG, respectively). The same happened with the SV, but the recovery of this parameter in the NTG was more pronounced after the AMI than in the TG, with a mean overall increase of 0.03 and 0.06 mL (for NTG and TG, respectively). The estimated LV mass seemed not to be affected by the AMI, but an increase in this parameter was observed over the study, with an overall increase of

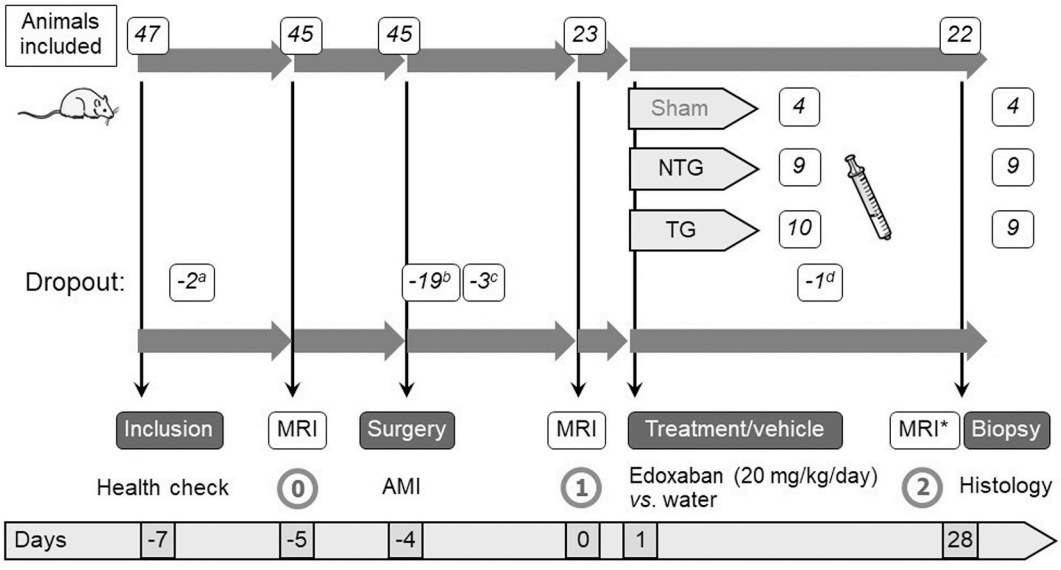

Fig. 1. Experimental design and workflow. Graphical representation of the experimental design with the linear workflow of the interventions, analysis, and the animals included and dropouts. Abbreviations: AMI: acute myocardial infarction; MRI: cardiac magnetic resonance imaging; NTG: non-treated group; Sham: sham operated animals; TG: treated group. [a] No passing health check; [b] intraoperative mortality; [c] No support the infarction; [d] gastrointestinal bleeding. *Two animals of each group could not undergo MRI2 because COVID pandemic lockdown.

Table 2
Results from the MRI analysis during the study.

Variable	MRI*	NTG ($n = 9$)	TG ($n = 9$)	p^a
EDV (mL)	MRI0	0.70 ± 0.05	0.64 ± 0.05	0.805
	MRI1	0.67 ± 0.03	0.67 ± 0.05	0.945
	MRI2	0.77 ± 0.03	0.77 ± 0.06	0.805
p^b		0.734	0.196	
p^c		**0.042**	**0.028**	
p^d		**0.027**	**0.027**	
ESV (mL)	MRI0	0.35 ± 0.05	0.30 ± 0.03	0.456
	MRI1	0.36 ± 0.04	0.32 ± 0.03	0.295
	MRI2	0.39 ± 0.02	0.38 ± 0.05	0.710
p^b		0.600	0.463	
p^c		0.236	0.108	
p^d		0.399	0.072	
SV (mL)	MRI0	0.35 ± 0.01	0.34 ± 0.02	1.000
	MRI1	0.31 ± 0.02	0.35 ± 0.04	0.731
	MRI2	0.38 ± 0.02	0.40 ± 0.02	0.535
p^b		0.233	0.292	
p^c		**0.027**	**0.017**	
p^d		**0.027**	0.172	
EF (%)	MRI0	50.47 ± 2.57	53.20 ± 1.25	0.456
	MRI1	46.74 ± 3.42	52.53 ± 3.02	0.534
	MRI2	49.84 ± 1.57	52.30 ± 3.20	0.710
p^b		**0.028**	0.917	
p^c		0.499	0.499	
p^d		0.735	0.345	
e-LVM (g)	MRI0	0.56 ± 0.02	0.54 ± 0.02	0.620
	MRI1	0.59 ± 0.03	0.59 ± 0.03	0.731
	MRI2	0.61 ± 0.03	0.60 ± 0.03	0.805
p^b		0.395	0.068	
p^c		**0.034**	**0.034**	
p^d		0.352	0.891	

Data from sham group are not presented since only MRI0 was done in this group and their values were like the other groups (no surgical interventions were done at this point).
* Two animals of each group could not undergo MRI2 because COVID pandemic lockdown.
[a] p value of the U Mann-Whitney test for the comparison between NTG and TG.
[b] p value of the Wilcoxon test for the comparison between MRI0 and MRI1.
[c] p value of the Wilcoxon test for the comparison between MRI0 and MRI2.
[d] p value of the Wilcoxon test for the comparison between MRI1 and MRI2.
Bold numbers indicate statistical significance.
Abbreviations: EDV: end-diastolic volume, EF: ejection fraction, e-LVM: estimated left ventricle mass, ESV: end-systolic volume, MRI: magnetic resonance imaging, NTG: non-treated group, SV: systolic volume, TG: treated group.

0.05 and 0.06 g (for NTG and TG, respectively).

AMI was confirmed in the MRI studies by LGE. We considered 'Probable' and 'Yes' as positive diagnostic categories in LGE for myocardial infarct, and 'No' and 'Possible' as negative diagnostic categories. We took as infarcts those myocardial scars which measured more than 5% of the LV surface in histology and no infarcts those myocardial scars which measured less than 5%. MRI1 had a 33% sensitivity, an 80% specificity, a 75% positive predictive value and a 40% negative predictive value, with an overall accuracy of 50%. MRI2 had a 22% sensitivity, a 100% specificity, a 100% positive predictive value and a 42% negative predictive value, with an overall accuracy of 50%.

No statistical difference in the detection of the AMI by LGE was observed between the NTG and TG at MRI1 ($p = 0.383$). No difference was observed between these groups at MRI2 ($p = 0.318$; Fig. 3A and B). Therefore, AMI sequelae in MRI were comparable for both groups. Finally, although the radiologist observer detected an improvement in LGE between MRI1 and MRI2 in three of seven rats in the NTG and five of seven rats of the TG, this difference was not statistically significant ($p = 0.280$; Fig. 3C). Four animals (two per group) could not complete the MRI2 because of the COVID-19 pandemic lockdown.

3.4. Histologic analysis after 28 days of treatment post-infarction

The wet weight of the hearts at the end of the study was 1.82 ± 0.08 g for the NTG and 2.02 ± 0.12 g for the TG, with no statistical difference between them ($p = 0.169$). In the same way, the ratio of weights between the hearts and animals was no different for both groups (0.49 ± 0.03 and 0.54 ± 0.03% for NTG and TG, respectively; $p = 0.215$).

In the histological analysis, we found small fibrotic areas located on the lateral LV wall in all individuals, that are compatible with well-healed small myocardial infarcts. The area of infarction was measured in the representative histological slides of the AMI, after Masson's staining, to optimise the image differentiation between healthy tissue and scar tissue (Fig. 4A). The area of infarction was automatically calculated by the 'Split channels' function (green channel) from Fiji-ImageJ® software (https://imagej.net/software/fiji/).

Assuming a threshold of 5% of scarred myocardial surface in histological slices to consider the infarct as significative, we obtained that 72.2% of animals surpassed that threshold and presented significative AMI (77.7 and 66.6 % for TG and NTG, respectively, $p > 0.05$).

Scars were located in the lateral wall of the LV, as expected after the ligature of the LAD artery in rats. Mean infarcted myocardial surfaces were 6.3 ± 3.2 and 14.6 ± 6.5 mm^2, for NTG and TG, respectively ($p = 0.536$). The percentage of the infarcted area over the total area of the heart section was 9.1 ± 2.7 and 11.4 ± 3.4% for NTG and TG, respectively ($p = 0.514$; Fig. 4B). A good correlation was observed between the infarcted area denoted by LGE and the scar observed in the histological analysis (Fig. 4C), which validated the data obtained by cardiac MRI.

Haemorrhagic level in the ventricle wall, leukocyte infiltration, ventricle wall thinning, depth of the infarct in the ventricle wall, and necrosis were evaluated and categorised in the haematoxylin–eosin staining of all the hearts. Leukocyte infiltration was only valued as presenr or not, depth of infarct was categorised as transmural or not, and the rest of the variables were valued on a three-grade scale (mild, moderate, and severe). The results of this analysis are summarised in Supplementary Table S1. Specific staining and immunohistological analysis were done over the slides with infarction. Masson's staining served to evaluate the dimension of the infarction-induced scar. The expression of different biomarkers was revealed by immunohistological analysis to characterise the cardiac tissue. The following proteins were analysed in three regions (core, periphery, and surroundings) with respect to the infarct lesions: desmin (marker of myofilaments), vimentin (marker of fibroblasts), α-SMA (marker of myofibroblast and/or smooth muscle cells), VEGF (angiogenic and pro-remodelling factor), MMP9 (remodelling protease), TIMP1 (metalloproteases inhibitor), SOD2 (antioxidant enzyme), and TGFβ1 (profibrotic marker). Core was defined as the area clearly affected by the infarct, and where it was possible to demonstrate the formation of collagen histologically (Masson's staining), the loss of desmin or the formation of vimentin. Periphery was considered the thin layer bordering the core, where changes in the normal histology of the heart were evident. Finally, the surroundings were defined as the area bordering the periphery zone and where the histologic disposition of the tissue was a transition between the infarct zone and the normal tissue.

Staining patterns were evaluated using the intact myocardial tissue present in all slides as an internal control. Staining or immunohistological patterns were graded as Grade 0: no staining, Grade 1: much less detectable, Grade 2: slightly less detectable, Grade 3: detectable at the same level as intact myocardium, Grade 4: slightly more detectable, and Grade 5: much more detectable. The results of the immunohistological analysis are summarised in Supplementary Table S1.

As a result, a tendency to a higher necrosis level was observed ($p = 0.067$) in the peri-infarcted area of the TG with respect to the NTG, but no changes were detected for SOD2 (Fig. 5). VEGF expression in the peripheral area of the infarction was significantly less in the TG than in the NTG ($p = 0.027$). However, this was not associated with significant changes in α-SMA expression. Desmin expression was slightly higher in

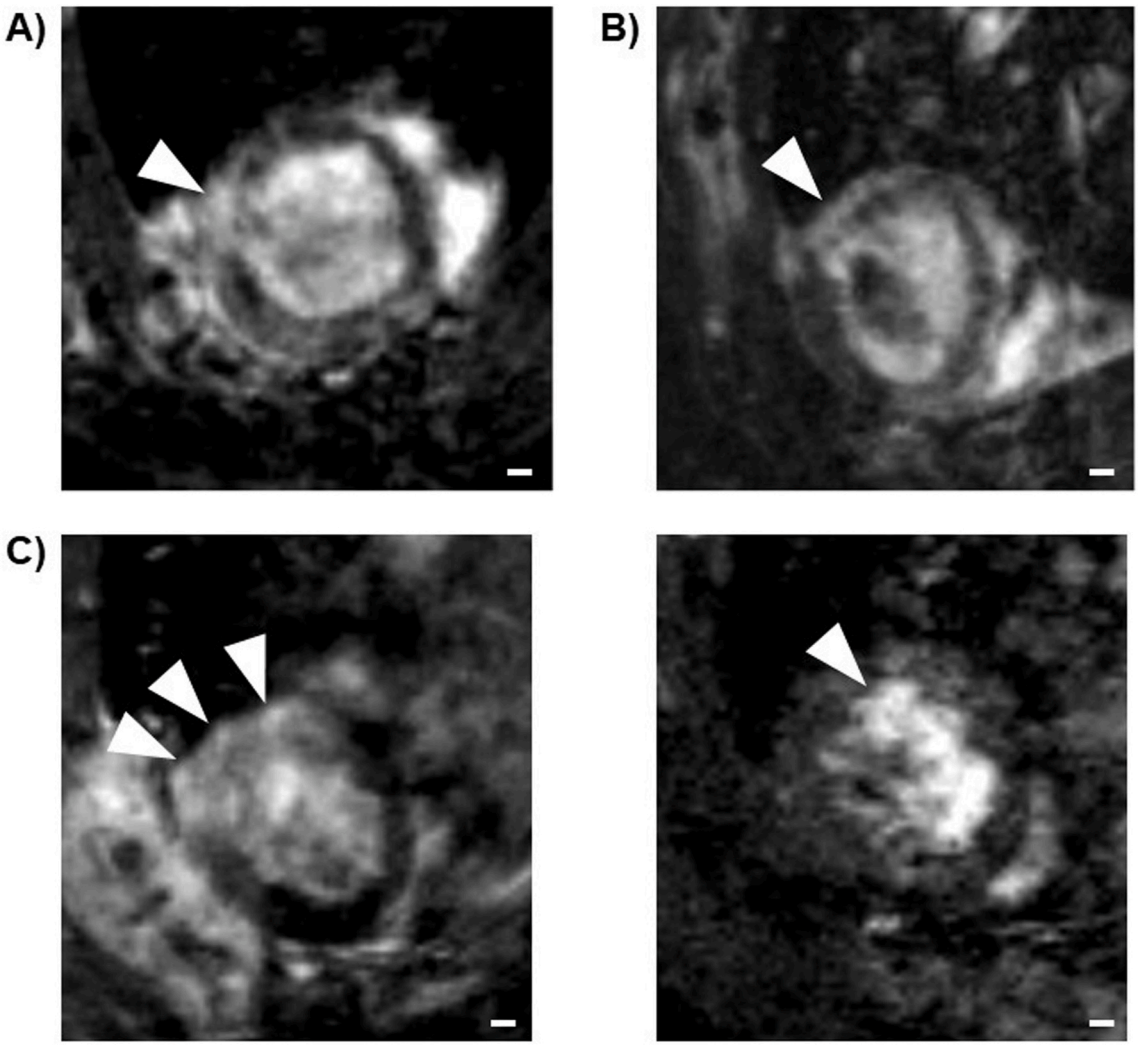

Fig. 3. Cardiac MRI study. Representative images of late gadolinium enhancement (LGE) for (**A**), an animal of the treated group, and (**B**) an animal from the non-treated group, in the moment of the MRI at the end of the study. (**C**) An example of improvement of myocardial scar observed in the MRI study for a treated animal. Left image shows a representative LGE after infarction induction (MRI1), and right image at 28 days post-treatment (MRI2). White arrows point to myocardial infarct regions. Scale bars = 1 mm.

the surrounding regions of the TG, and there could be a possible reduction of TGFβ1 and MMP9 expression in the core and periphery of the TG, respectively (Fig. 5). However, no differential expression was observed for vimentin or TIMP1 between the NTG and TG. These data merit a discussion about the possibility of a modification in the fibrosis process in the TG.

4. Discussion

In this work, an experimental method has been successfully developed to assess the post-MI remodelling in rats over 4 weeks. The method was based on cardiac MRI in living animals and a final histological analysis of the hearts. The influence of a treatment with daily oral edoxaban (20 mg/kg/day) in post-infarcted rats during the follow-up period was analysed and compared with non-treated animals. To our knowledge, this was done for the first time. In our experimental model, this treatment was not shown to be deleterious. The risk of bleeding was in a reasonable range, as shown by no external signs of bleeding during the treatment. Only one animal died of internal damage induced by the intragastric gavage, but not directly by the treatment. Thus, good data on safety was observed. The general physical recovery of treated animals was better than non-treated animals during the follow-up period. Although there was not a marked effect of edoxaban in the post-infarction heart remodelling, a possible weak reduction of fibrosis, shown by a significant reduction of VEGF, and a tendency to less TGFβ1 and MMP9 expression, was observed. Overall data suggested non-inferiority of edoxaban compared to placebo, and in some parameters, edoxaban could be beneficial for heart recovery during the mid-term post-MI period.

The intraoperative and perioperative mortality rates of our study were similar to previous reports in this experimental model (Antonio et al., 2009; Lin et al., 2008; Pfeffer et al., 1979). EDV, ESV, SV and EF were mostly unaffected by AMI onset, findings that are in agreement with previous reports (Pfeffer et al., 1979). On the contrary, EDV and SV increased during the post-infarction follow-up period, maintaining the global values of EF in both the NTG and TG. Only EF was reduced after infarction in some rats, and this parameter was not totally recovered during the follow-up time, although the mean values did not worsen in the TG or NTG. Evolution of estimated LV mass in MRIs and heart mass at necropsy showed no significant myocardial mass lost during the overall process. Total weight gain during the follow-up was always continuous, showing the recovery of the general state of the animals. These findings are in accordance with previous works (Pfeffer et al., 1979), concluding that the rat model of coronary artery ligation does not

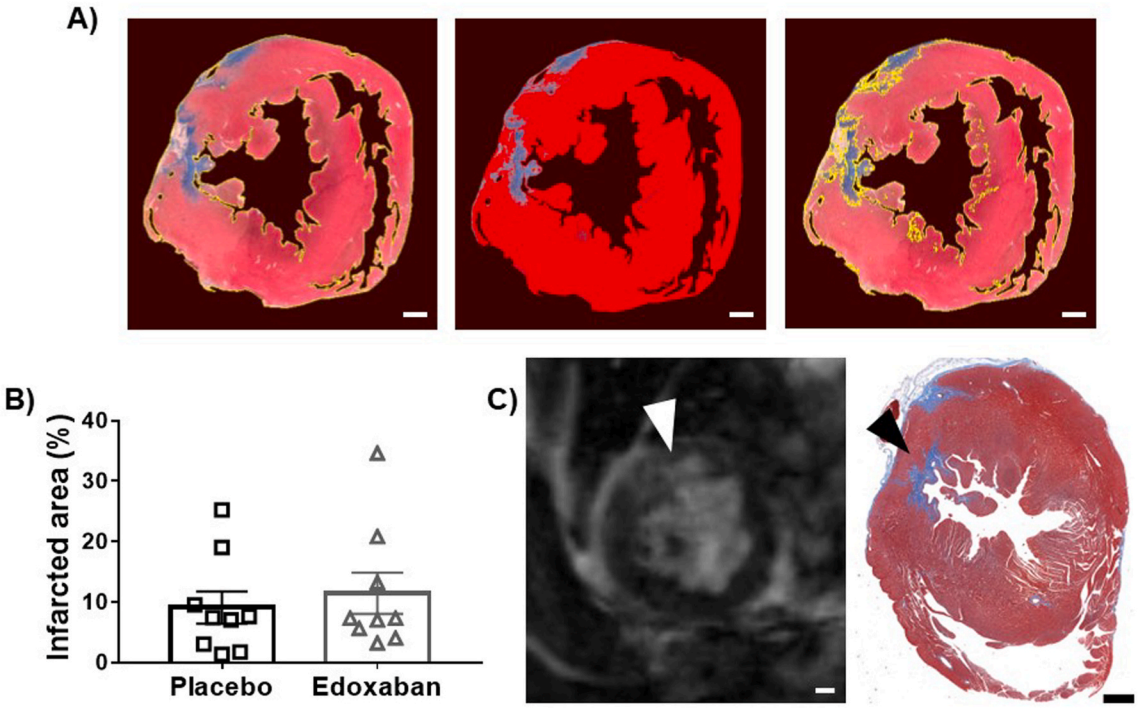

Fig. 4. Infarct characterization. (**A**) Representative images of Masson's staining in an infarcted section, showing the steps for the calculus of the infarcted area: from left to right, the images show 1) the total area of the heart section bounded by a yellow line, 2) the computational contrast differentiation for infarction differentiation, and 3) the area of heart free of infarction bounded by a yellow line. (**B**) Mean of the infarcted area on the non-treated group (NTG, placebo) and treated group (TG). Columns represent the mean value of the group and symbols show the individual values of each animal. (**C**) Left image shows an example of the MRI of late gadolinium enhancement, and right image shows the histological image after Masson's trichrome staining of the same region of the heart at the end of the study. Arrows mark the site of correlation in both images. Scale bars = 1 mm.

produce gross heart failure. In this sense, although the permanent ligation of the coronary artery is not the most mimetical model of the clinical situation in humans, where the opening of the coronary flow is a mandatory objective, the particularity of the rats to support the infarcts makes them suitable to study myocardial recovery and remodelling after AMI.

The evolution of cardiac function after LAD coronary artery ligation was unaffected by the treatment with edoxaban. There were no statistical differences in any parameter of the cardiac MRI analysis (EDV, SV, estimated LV mass, and EF) after the period of treatment between the NTG and the TG. It deserves comment that we detected five cases of improvement in the LGE image after the treatment with edoxaban and only three cases in the NTG. However, we could not perform the final MRI in four animals, because of the pandemic lockdown, and this drastically reduced our statistical power, and as a result, no significance was reached. Therefore, cardiac function, analysed by MRI, was unaffected by the treatment of edoxaban in our experimental conditions. This means that there was no worsening of this function: cardiac toxicity or damage was not produced by edoxaban. However, it would be of interest to analyse a possible improvement in cardiac function by post-MI edoxaban treatment in a larger study.

Histology confirmed that the surgical procedure was effective in creating a myocardial scar in all animals, with 72.2% of them of significant size, these results being similar to those obtained by Pfeffer et al. (1979). The mean infarcted myocardial surface was 10.2 ± 3.5%, lower than data reported by Kainuma et al. (2017), which obtained 29%, but also with a great variation (from 4 to 65%) and using female Lewis rats, not male Wistar–Kyoto as in our case. Furthermore, we have calculated the percentage of the infarcted area, in comparison to all the heart surfaces in the section, not only the LV area. All lesions were located in the lateral wall of the LV, confirming the ligature of the LAD artery, which is described to irrigate that area at least in some other strains (Kainuma et al., 2017). LGE findings were consistent with the histological location of AMI scars, with a 50% global diagnostic accuracy, still lesser than observed in human diagnostic MRI (Kim et al., 2008; Ordovas and Higgins, 2011), probably because of the small size of the heart and infarct.

Edoxaban (20 mg/kg/day) was administered daily by an intragastric gavage in an aqueous solution. Water was administered in control animals by the same procedure, in the same volume as in the treated group. Rats supported the manoeuvre, but attention should be taken to avoid the unexpected movements of the animal during administration, especially in treated rats. The reason is that any violent movement could damage the oesophagus or stomach of the animal and induce internal bleeding. This happened with one of the animals treated with edoxaban, and it died less than 24 h after the damage. Because the bleeding was internal, it was undetectable until autopsy. However, it was the only case of bleeding, which allows us to conclude that the procedure of intragastric gavage and the dosage of edoxaban is, with a controllable risk, safe for rats. As observed in clinical trials, edoxaban is not exempted from bleeding risk, but the overall rate of bleeding-related problems is reduced comparing to traditional anticoagulants like vitamin K antagonists (Vilain et al., 2020; Zelniker et al., 2019). The long-term effects of edoxaban therapy in patients with atrial fibrillation and stable coronary artery disease are currently under study (Cho et al., 2022).

Anticoagulant treatment was maintained for 28 days in parallel with placebo. During this time, animals recovered from the AMI and general health conditions were followed by daily weighing. This allowed us to confirm the recovery of all the animals but with a significant improvement in the TG with respect to the NTG and sham group. Interestingly, survival from myocardial infarct seemed to induce a general reaction in the animals observed by a rapid body weight gain from day 4 after the event and during the following 10 days. After that, body weight increase was parallel to the NTG and sham groups. Weight gain in the TG seemed to be faster from day 11 of treatment in comparison with the NTG and

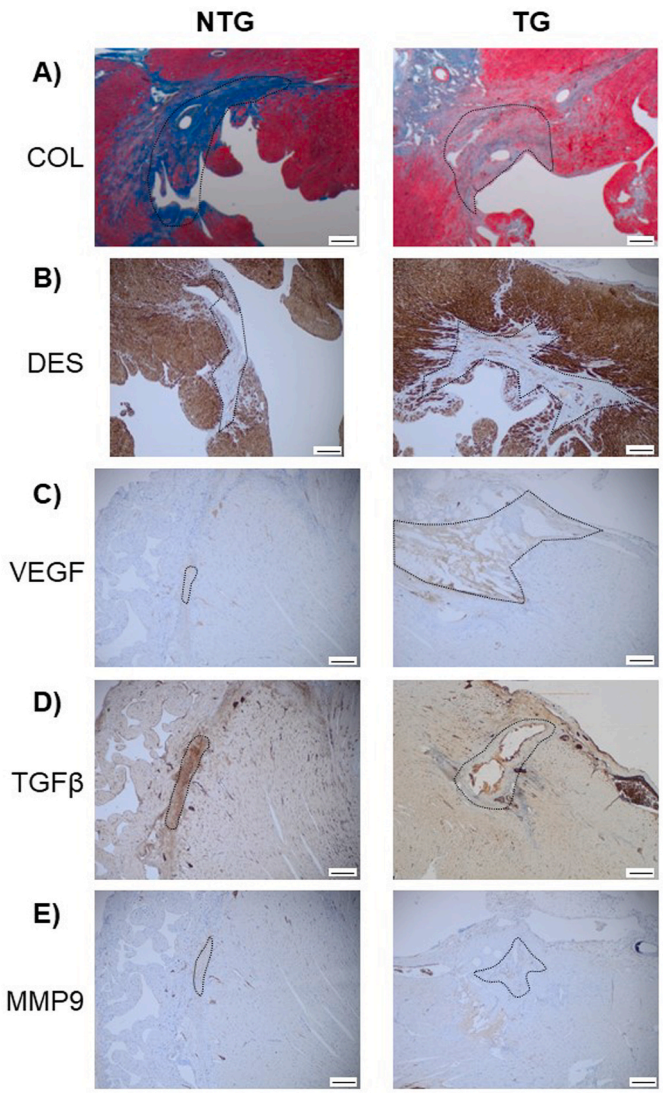

Fig. 5. Histological analysis. Representative histological images (all acquired at 4×) of infarct regions in the hearts from the non-treated group (NTG, left column of images) or from the treated group (TG, right column) of animals, after staining with Masson's trichrome and immunostainings with different antibodies. (**A**) Masson's trichrome staining (COL), which show higher necrosis in the periinfarcted area of the TG. Collagen is stained in blue, muscle in red and necrosis in light red/pink (**B**) Desmin (DES) expression was slightly higher in the surrounding regions of TG. Positive staining in brown. (**C**) VEGF expression in the peripheral area of the infarction was significantly less in TG than in NTG. Positive staining in brown. (**D**) Possibly a reduction of TGFβ1 expression in the infarct core of TG. Positive staining in brown. (**E**) Reduction of MMP9 expression in the periphery area of TG. Positive staining in brown. Dotted lines showing the core of the infarct regions. Scale bars = 250 μm.

sham, and this healthy state could be due to edoxaban treatment. Large studies in the elderly have been done with edoxaban, and it has become the Fit-fOR-The-Aged (FORTA) classification of beneficial (B level). However, its vote was closest to very beneficial (A level) (Wehling et al., 2017). This underlines the overall positive assessment of the risk/benefit ratio for this drug against available evidence.

Post-infarction treatment with edoxaban for 28 days did not have a remarkable effect on cardiac remodelling in our experiments. This period of 4 weeks was previously used in rat models for the evaluation of post-MI cardiac remodelling (Lin et al., 2008; Liu et al., 2009; Saleh et al., 2012), and this was the reason to maintain the treatment during that time. We could also confirm that animals were able to recover their general physical state in that period. The histological analysis of the biopsies allowed a detailed study of the remodelling process. As stated, there was no change in the size of the infarction after treatment. However, this was something expected, considering the nature of this end-point parameter. Analysing by biomarkers, the absence of differences in α-SMA and vimentin expression between the NTG and TG suggests that after 28 days of treatment, edoxaban was not able to reduce fibroblast migration to the scar. The conversion of fibroblasts to myofibroblasts can be followed by the expression of α-SMA (Venugopal et al., 2022), and its presence suggests the activation of the secretion of extracellular matrix components to the scar of the damaged tissue. A process that seems to be still active after 28 days post-infarction, independently of the edoxaban treatment.

Cardiac remodelling also seems to be active after edoxaban treatment. The immunohistochemistry for vimentin reveals all the non-myocardial cell types, including endothelial cells, vascular smooth muscle, fibroblasts, etc. Therefore, its positivity suggests the location of active remodelling (Kondo et al., 2022). However, this could also suggest that this remodelling could be a mechanism to avoid the formation of a permanent scar with reduced contractile properties, since myocardial fibrosis areas did not reveal myofibroblasts in previous works (Istratoaie et al., 2015). In fact, in our samples, there was a slightly higher expression of desmin in the surroundings of the scar in the TG. This element of the myofilaments could indicate better protection of cardiomyocytes by the action of edoxaban. This protein has been found in the late period after infarction during the remodelling process (Datta et al., 2017).

Although the levels of TIMP1 were not affected comparing TG and NTG, the possible tendency to the reduction of TGFβ1 and MMP9 shown in the TG could also suggest reduced fibrosis after 28 days of treatment, through the TGFβ1-Smad-MMP9 signalling pathway (Wang et al., 2022). The active participation of MMPs in the remodelling process of rat hearts has been previously demonstrated (Parthasarathy et al., 2014). This could be supported by the fact of the reduction observed in VEGF expression in the periphery of the infarction of the TG with respect to NTG, which could suggest a reduced active process of remodelling after 28 days of treatment (Cheng et al., 2016). Results agree with the possible anti-inflammatory and protective effects showed by edoxaban in endothelial cells, which could have a role in the protection and recovery of cardiac tissue (Almenglo et al., 2020). More recently, it has been demonstrated that DOAC, apart from their anticoagulant effects, also have cellular effects affecting gene expression, inflammatory response, and fibrosis (Gadi et al., 2021). These effects are more pronounced for FXa inhibitors than for thrombin inhibitors and depend, at least in part, on the different activation of protein C, a signal component and cytoprotective protease.

Finally, oxidative stress has been suggested to participate in cardiac remodelling after AMI in murine models (Hou et al., 2018). A reduction in superoxide anions by SOD or hydrogen peroxide by catalase could reduce the tissue damage caused by ischaemia. However, there were no changes in SOD2 levels between the NTG and TG, in agreement with previous studies (Almeida et al., 2014).

4.1. Limitations

The main limitation of our study is the number of animals included in the study. This reduces the potency of the statistical analysis. The variation of the infarct size induced by the experimental model contributes to this limitation. Further research in large populations is needed to confirm our findings. Second, our study was made only in males of a particular rat strain; thus, the results can be different considering sex and strain differences. Third, the last MRI (MRI2) was not possible in some of the animal, because the irruption of the SARS-CoV-2 pandemic situation closed some facilities in our institute.

4.2. Conclusions

In conclusion, our surgical protocol showed effectiveness in creating an AMI and the radiological and histological results provide some experimental basis to support the feasibility of MRI to study cardiac function and characterise myocardial scars in a rat model. However, further *in vivo* studies should be developed especially to improve the homogeneity of infarcts and, thus, improve the LGE diagnostic sequence performance.

For the first time in our model, daily oral edoxaban treatment after infarction was shown to be safe, with a controllable risk of bleeding. In comparison to the placebo, edoxaban showed a better general recovery of animals, non-inferiority heart remodelling, and promising data in pathophysiological modulation of cardiac fibrosis and angiogenesis. Therefore, the present results justify further research on post-infarction cardiac recovery by edoxaban treatment. Especially trying to exploit the possible benefit of pharmacological modulation of adverse cardiac remodelling.

Financial support

This work was supported by Daiichi-Sankyo Spain.

Funding for open access charge: Universidade de Santiago de Compostela/CISUG

CRediT authorship contribution statement

Javier Martínez-Fernández: Investigation, Formal analysis, Writing – original draft, Writing – review & editing. **Cristina Almengló:** Investigation, Formal analysis, Writing – original draft, Writing – review & editing. **Borja Babarro:** Investigation. **Ramón Iglesias-Rey:** Investigation, Formal analysis, Writing – review & editing. **Tomás García-Caballero:** Investigation, Formal analysis. **Ángel L. Fernández:** Investigation. **Miguel Souto-Bayarri:** Conceptualization, Supervision, Funding acquisition, Investigation, Formal analysis, Writing – review & editing. **José R. González-Juanatey:** Conceptualization, Supervision, Funding acquisition, Investigation, Formal analysis. **Ezequiel Álvarez:** Conceptualization, Supervision, Funding acquisition, Investigation, Formal analysis, Writing – review & editing.

Declaration of competing interest

The authors declare the following financial interests/personal relationships which may be considered as potential competing interests:

Authors declare that this work was supported by Daiichi-Sankyo España, but this did not influence the results or interpretation of this manuscript for any of the authors.

Data availability

Data will be made available on request.

Acknowledgements

Thanks to María Otero Alen, by the processing of histological samples in the Immunohistochemistry Lab of the Health Research Institute of Santiago de Compostela.

Appendix A. Supplementary data

Supplementary data to this article can be found online at https://doi.org/10.1016/j.ejphar.2023.176216.

References

Ahmed, N., Carrick, D., Layland, J., Oldroyd, K.G., Berry, C., 2012. The role of cardiac magnetic resonance imaging (MRI) in acute myocardial infarction (AMI). Heart Lung Circ. 22, 243–255. S1443-9506(12)01392-3 [pii]10.1016/j.hlc.2012.11.016.

Almeida, S.A., Claudio, E.R., Mengal, V., Oliveira, S.G., Merlo, E., Podratz, P.L., Gouvea, S.A., Graceli, J.B., de Abreu, G.R., 2014. Exercise training reduces cardiac dysfunction and remodeling in ovariectomized rats submitted to myocardial infarction. PLoS One 9, e115970. https://doi.org/10.1371/journal.pone.0115970PONE-D-14-27279 [pii].

Almenglo, C., Mosquera-Garrote, N., Gonzalez-Peteiro, M., Gonzalez-Juanatey, J.R., Alvarez, E., 2020. Edoxaban's contribution to key endothelial cell functions. Biochem. Pharmacol. 178, 114063. S0006-2952(20)30297-5 [pii]10.1016/j.bcp.2020.114063.

Antonio, E.L., Dos Santos, A.A., Araujo, S.R., Bocalini, D.S., Dos Santos, L., Fenelon, G., Franco, M.F., Tucci, P.J., 2009. Left ventricle radio-frequency ablation in the rat: a new model of heart failure due to myocardial infarction homogeneous in size and low in mortality. J. Card. Fail. 15, 540–548. S1071-9164(09)00029-3 [pii]10.1016/j.cardfail.2009.01.007.

Ardissino, D., Merlini, P.A., Bauer, K.A., Galvani, M., Ottani, F., Franchi, F., Bertocchi, F., Rosenberg, R.D., Mannucci, P.M., 2003. Coagulation activation and long-term outcome in acute coronary syndromes. Blood 102, 2731–2735. https://doi.org/10.1182/blood-2002-03-0954S0006-4971(20)50416-3 [pii].

Capodanno, D., Bhatt, D.L., Eikelboom, J.W., Fox, K.A.A., Geisler, T., Michael Gibson, C., Gonzalez-Juanatey, J.R., James, S., Lopes, R.D., Mehran, R., Montalescot, G., Patel, M., Steg, P.G., Storey, R.F., Vranckx, P., Weitz, J.I., Welsh, R., Zeymer, U., Angiolillo, D.J., 2020. Dual-pathway inhibition for secondary and tertiary antithrombotic prevention in cardiovascular disease. Nat. Rev. Cardiol. https://doi.org/10.1038/s41569-019-0314-y, 10.1038/s41569-019-0314-y.

Cheng, C., Li, P., Wang, Y.G., Bi, M.H., Wu, P.S., 2016. Study on the expression of VEGF and HIF-1alpha in infarct area of rats with AMI. Eur. Rev. Med. Pharmacol. Sci. 20, 115–119.

Cho, M.S., Kang, D.Y., Oh, Y.S., Lee, C.H., Choi, E.K., Lee, J.H., Kwon, C.H., Park, G.M., Park, H.W., Park, K.H., Park, K.M., Hwang, J., Yoo, K.D., Cho, Y.R., Kim, Y.R., Hwang, K.W., Jin, E.S., Kim, P.J., Kim, K.H., Park, D.W., Nam, G.B., 2022. Edoxaban-based long-term antithrombotic therapy in patients with atrial fibrillation and stable coronary disease: rationale and design of the randomized EPIC-CAD trial. Am. Heart J. 247, 123–131. S0002-8703(22)00023-0 [pii]10.1016/j.ahj.2022.01.014.

Datta, K., Basak, T., Varshney, S., Sengupta, S., Sarkar, S., 2017. Quantitative proteomic changes during post myocardial infarction remodeling reveals altered cardiac metabolism and Desmin aggregation in the infarct region. J. Proteonomics 152, 283–299. S1874-3919(16)30498-5 [pii]10.1016/j.jprot.2016.11.017.

Deitelzweig, S., Bergrath, E., di Fusco, M., Kang, A., Savone, M., Cappelleri, J.C., Russ, C., Betts, M., Cichewicz, A., Schaible, K., Tarpey, J., Fahrbach, K., 2022. Real-world evidence comparing oral anticoagulants in non-valvular atrial fibrillation: a systematic review and network meta-analysis. Future Cardiol. 18, 393–405. https://doi.org/10.2217/fca-2021-0120.

Do, H.P., Ramanan, V., Qi, X., Barry, J., Wright, G.A., Ghugre, N.R., Nayak, K.S., 2018. Non-contrast assessment of microvascular integrity using arterial spin labeled cardiovascular magnetic resonance in a porcine model of acute myocardial infarction. J. Cardiovasc. Magn. Reson. 20, 45. https://doi.org/10.1186/s12968-018-0468-5, 10.1186/s12968-018-0468-5 [pii].

Fawzy, A.M., Yang, W.Y., Lip, G.Y., 2019. Safety of direct oral anticoagulants in real-world clinical practice: translating the trials to everyday clinical management. Expet Opin. Drug Saf. 18, 187–209. https://doi.org/10.1080/14740338.2019.1578344.

Gadi, I., Fatima, S., Elwakiel, A., Nazir, S., Mohanad Al-Dabet, M., Rana, R., Bock, F., Manoharan, J., Gupta, D., Biemann, R., Nieswandt, B., Braun-Dullaeus, R., Besler, C., Scholz, M., Geffers, R., Griffin, J.H., Esmon, C.T., Kohli, S., Isermann, B., Shahzad, K., 2021. Different DOACs control inflammation in cardiac ischemia-reperfusion differently. Circ. Res. 128, 513–529. https://doi.org/10.1161/CIRCRESAHA.120.317219.

Garg, P., Saunders, L.C., Swift, A.J., Wild, J.M., Plein, S., 2018. Role of cardiac T1 mapping and extracellular volume in the assessment of myocardial infarction. Anatol. J. Cardiol. 19, 404–411. https://doi.org/10.14744/AnatolJCardiol.2018.39586.

Heiberg, E., Sjogren, J., Ugander, M., Carlsson, M., Engblom, H., Arheden, H., 2010. Design and validation of Segment–freely available software for cardiovascular image analysis. BMC Med. Imag. 10, 1, 1471-2342-10-1 [pii]10.1186/1471-2342-10-1.

Hou, L., Guo, J., Xu, F., Weng, X., Yue, W., Ge, J., 2018. Cardiomyocyte dimethylarginine dimethylaminohydrolase1 attenuates left-ventricular remodeling after acute myocardial infarction: involvement in oxidative stress and apoptosis. Basic Res. Cardiol. 113, 28. https://doi.org/10.1007/s00395-018-0685-y, 10.1007/s00395-018-0685-y [pii].

Istratoaie, O., OfiTeru, A.M., Nicola, G.C., Radu, R.I., Florescu, C., Mogoanta, L., Streba, C.T., 2015. Myocardial interstitial fibrosis - histological and immunohistochemical aspects. Rom. J. Morphol. Embryol. 56, 1473–1480, 56041514731480[pii].

Kainuma, S., Miyagawa, S., Fukushima, S., Tsuchimochi, H., Sonobe, T., Fujii, Y., Pearson, J.T., Saito, A., Harada, A., Toda, K., Shirai, M., Sawa, Y., 2017. Influence of coronary architecture on the variability in myocardial infarction induced by coronary ligation in rats. PLoS One 12, e0183323. https://doi.org/10.1371/journal.pone.0183323PONE-D-17-16631 [pii].

Keeley, E.C., Boura, J.A., Grines, C.L., 2003. Primary angioplasty versus intravenous thrombolytic therapy for acute myocardial infarction: a quantitative review of 23 randomised trials. Lancet 361, 13–20. S0140-6736(03)12113-7 [pii]10.1016/S0140-6736(03)12113-7.

Khan, M.A., Hashim, M.J., Mustafa, H., Baniyas, M.Y., Al Suwaidi, S.K.B.M., AlKatheeri, R., Alblooshi, F.M.K., Almatrooshi, M.E.A.H., Alzaabi, M.E.H., Al Darmaki, R.S., Lootah, S.N.A.H., 2020. Global epidemiology of ischemic heart disease: results from the global burden of disease study. Cureus 12, e9349. https://doi.org/10.7759/cureus.9349.

Kim, R.J., Albert, T.S., Wible, J.H., Elliott, M.D., Allen, J.C., Lee, J.C., Parker, M., Napoli, A., Judd, R.M., 2008. Performance of delayed-enhancement magnetic resonance imaging with gadoversetamide contrast for the detection and assessment of myocardial infarction: an international, multicenter, double-blinded, randomized trial. Circulation 117, 629–637. CIRCULATIONAHA.107.723262 [pii]10.1161/CIRCULATIONAHA.107.723262.

Klocke, R., Tian, W., Kuhlmann, M.T., Nikol, S., 2007. Surgical animal models of heart failure related to coronary heart disease. Cardiovasc. Res. 74, 29–38. S0008-6363(06)00514-1 [pii]10.1016/j.cardiores.2006.11.026.

Kondo, T., Takahashi, M., Yamasaki, G., Sugimoto, M., Kuse, A., Morichika, M., Nakagawa, K., Sakurada, M., Asano, M., Ueno, Y., 2022. Immunohistochemical analysis of vimentin expression in myocardial tissue from autopsy cases of ischemic heart disease. Leg. Med. 54, 102003. S1344-6223(21)00167-X [pii]10.1016/j.legalmed.2021.102003.

Li, J.H., Dai, J., Han, B., Wu, G.H., Wang, C.H., 2019. MiR-34a regulates cell apoptosis after myocardial infarction in rats through the Wnt/beta-catenin signaling pathway. Eur. Rev. Med. Pharmacol. Sci. 23, 2555–2562. https://doi.org/10.26355/eurrev_201903_17404.

Lin, J.F., Lin, S.M., Chih, C.L., Nien, M.W., Su, H.H., Hu, B.R., Huang, S.S., Tsai, S.K., 2008. Resveratrol reduces infarct size and improves ventricular function after myocardial ischemia in rats. Life Sci. 83, 313–317. S0024-3205(08)00241-5 [pii]10.1016/j.lfs.2008.06.016.

Liu, Y.H., D'Ambrosio, M., Liao, T.D., Peng, H., Rhaleb, N.E., Sharma, U., Andre, S., Gabius, H.J., Carretero, O.A., 2009. N-acetyl-seryl-aspartyl-lysyl-proline prevents cardiac remodeling and dysfunction induced by galectin-3, a mammalian adhesion/growth-regulatory lectin. Am. J. Physiol. Heart Circ. Physiol. 296, H404–H412, 00747.2008[pii] 10.1152/ajpheart.00747.2008.

Makam, R.C.P., Hoaglin, D.C., McManus, D.D., Wang, V., Gore, J.M., Spencer, F.A., Pradhan, R., Tran, H., Yu, H., Goldberg, R.J., 2018. Efficacy and safety of direct oral anticoagulants approved for cardiovascular indications: systematic review and meta-analysis. PLoS One 13, e0197583. https://doi.org/10.1371/journal.pone.0197583PONE-D-17-40359 [pii].

Malliaras, K., Smith, R.R., Kanazawa, H., Yee, K., Seinfeld, J., Tseliou, E., Dawkins, J.F., Kreke, M., Cheng, K., Luthringer, D., Ho, C.S., Blusztajn, A., Valle, I., Chowdhury, S., Makkar, R.R., Dharmakumar, R., Li, D., Marban, L., Marban, E., 2013. Validation of contrast-enhanced magnetic resonance imaging to monitor regenerative efficacy after cell therapy in a porcine model of convalescent myocardial infarction. Circulation 128, 2764–2775. CIRCULATIONAHA.113.002863 [pii]10.1161/CIRCULATIONAHA.113.002863.

Orbe, J., Zudaire, M., Serrano, R., Coma-Canella, I., Martinez de Sizarrondo, S., Rodriguez, J.A., Paramo, J.A., 2008. Increased thrombin generation after acute versus chronic coronary disease as assessed by the thrombin generation test. Thromb. Haemostasis 99, 382–387, 08020382 [pii]10.1160/TH07-07-0443.

Ordovas, K.G., Higgins, C.B., 2011. Delayed contrast enhancement on MR images of myocardium: past, present, future. Radiology 261, 358–374, 261/2/358 [pii]10.1148/radiol.11091882.

Parthasarathy, A., Gopi, V., Devi, K.M.S., Balaji, N., Vellaichamy, E., 2014. Aminoguanidine inhibits ventricular fibrosis and remodeling process in isoproterenol-induced hypertrophied rat hearts by suppressing ROS and MMPs. Life Sci. 118, 15–26. S0024-3205(14)00822-4 [pii]10.1016/j.lfs.2014.09.030.

Pfeffer, M.A., Pfeffer, J.M., Fishbein, M.C., Fletcher, P.J., Spadaro, J., Kloner, R.A., Braunwald, E., 1979. Myocardial infarct size and ventricular function in rats. Circ. Res. 44, 503–512. https://doi.org/10.1161/01.res.44.4.503.

Pop, C., Matei, C., Petris, A., 2019. Anticoagulation in acute coronary syndrome: review of major therapeutic advances. Am. J. Therapeut. 26, e184–e197. https://doi.org/10.1097/MJT.0000000000000091300045391-201904000-00002 [pii].

Saleh, M.G., Sharp, S.K., Alhamud, A., Spottiswoode, B.S., van der Kouwe, A.J., Davies, N.H., Franz, T., Meintjes, E.M., 2012. Long-term left ventricular remodelling in rat model of nonreperfused myocardial infarction: sequential MR imaging using a 3T clinical scanner. J. Biomed. Biotechnol. 2012, 504037 https://doi.org/10.1155/2012/504037.

Sharma, A., Garg, A., Borer, J.S., Krishnamoorthy, P., Garg, J., Lavie, C.J., Arbab-Zadeh, A., Mukherjee, D., Ahmad, H., Lichstein, E., 2014. Role of oral factor Xa inhibitors after acute coronary syndrome. Cardiology 129, 224–232, 000368747[pii]10.1159/000368747.

Shudo, Y., Miyagawa, S., Fukushima, S., Saito, A., Kawaguchi, N., Matsuura, N., Sawa, Y., 2011. Establishing new porcine ischemic cardiomyopathy model by transcatheter ischemia-reperfusion of the entire left coronary artery system for preclinical experimental studies. Transplantation 92, e34–e35. https://doi.org/10.1097/TP.0b013e31822d875c00007890-201110150-00024 [pii].

Venugopal, H., Hanna, A., Humeres, C., Frangogiannis, N.G., 2022. Properties and functions of fibroblasts and myofibroblasts in myocardial infarction. Cells 11 cells11091386[pii]10.3390/cells11091386.

Vilain, K., Li, H., Kwong, W.J., Antman, E.M., Ruff, C.T., Braunwald, E., Cohen, D.J., Giugliano, R.P., Magnuson, E.A., 2020. Cardiovascular- and bleeding-related Hospitalization rates with edoxaban versus warfarin in patients with atrial fibrillation based on results of the ENGAGE AF-TIMI 48 trial. Circ Cardiovasc Qual Outcomes 13, e006511. https://doi.org/10.1161/CIRCOUTCOMES.120.006511.

Wang, J., Wang, M., Lu, X., Zhang, Y., Zeng, S., Pan, X., Zhou, Y., Wang, H., Chen, N., Cai, F., Biskup, E., 2022. IL-6 inhibitors effectively reverse post-infarction cardiac injury and ischemic myocardial remodeling via the TGF-beta1/Smad3 signaling pathway. Exp. Ther. Med. 24, 576. https://doi.org/10.3892/etm.2022.11513ETM-24-3-11513 [pii].

Wehling, M., Collins, R., Gil, V.M., Hanon, O., Hardt, R., Hoffmeister, M., Monteiro, P., Quinn, T.J., Ropers, D., Sergi, G., Verheugt, F.W.A., 2017. Appropriateness of oral anticoagulants for the long-term treatment of atrial fibrillation in older people: results of an evidence-based review and international consensus validation process (OAC-FORTA 2016). Drugs Aging 34, 499–507. https://doi.org/10.1007/s40266-017-0466-6, 10.1007/s40266-017-0466-6 [pii].

World Health Organization, 2020. Global Health Estimates 2019: Deaths by Cause, Age, Sex, by Country and by Region, 2000-2019. https://www.who.int/data/global-health-estimates. (Accessed 27 March 2023).

Yla-Herttuala, E., Laidinen, S., Laakso, H., Liimatainen, T., 2018. Quantification of myocardial infarct area based on TRAFFn relaxation time maps - comparison with cardiovascular magnetic resonance late gadolinium enhancement, T1rho and T2 in vivo. J. Cardiovasc. Magn. Reson. 20, 34. https://doi.org/10.1186/s12968-018-0463-x, 10.1186/s12968-018-0463-x [pii].

Zelniker, T.A., Ruff, C.T., Wiviott, S.D., Blanc, J.J., Cappato, R., Nordio, F., Mercuri, M.F., Lanz, H., Antman, E.M., Braunwald, E., Giugliano, R.P., 2019. Edoxaban in atrial fibrillation patients with established coronary artery disease: insights from ENGAGE AF-TIMI 48. Eur Heart J Acute Cardiovasc Care 8, 176–185. https://doi.org/10.1177/2048872618790561.